Acoustic fields from PVDF interdigital transducers

P.D. Wilcox
P. Cawley
M.J.S. Lowe

Indexing terms: Interdigital transducers, PVDF, Lamb waves, Smart structures, Huygens' principle

Abstract: Interdigital transducers (IDTs) made from the piezoelectric polymer PVDF have been built; they transmit ultrasonic Lamb waves into 1–2 mm thick steel and aluminium plates and receive signals reflected from features in the structure. The IDTs are designed to be permanently bonded to the structure under inspection. Such IDTs have considerable potential for use in smart-structure monitoring applications. However, before this potential can be realised, the nature of the acoustic field that they produce must be thoroughly understood. Experimentally measured acoustic fields are presented for two example IDTs, one that produces a collimated beam for line inspection and one that produces a divergent beam for sector inspection. The development of modelling software based on Huygens' principle, which enables the acoustic field from such IDTs to be predicted rapidly, is then described. Example results from this software are presented and compared with experimental measurements. Further predictions made with the model are then used to elucidate certain basic guidelines for IDT design.

1 Introduction

Lamb waves are attractive for long-range inspection of plate-like structures, as a reasonable area of the structure can potentially be inspected by a transducer at a single location, as first suggested by Worlton [1]. A review of recent Lamb wave applications is given in [2], and the theoretical description can be found in Viktorov's text [3].

The excitation and detection of Lamb waves in structures can be achieved using a variety of devices, including interdigital transducers (IDTs), electromagnetic acoustic transducers (EMATs) [4] and wedge transducers [3, 5]. However, in smart-structure applications, a permanently attached device is required, and here IDTs have several advantages. First, they are low profile and unobtrusive compared with other types of Lamb wave transducer. Also, IDTs can be designed to have some degree of conformability, so that they can be used on convex or concave surfaces such as pipes and pressure vessels. However, it is the fact that the design of an IDT can be tailored to produce a variety of different shaped acoustic fields to suit the application that is the primary concern of this paper. For instance, IDTs have been constructed that transmit Lamb waves in a divergent pattern, and these could potentially be used to monitor a sector of a plate for defects such as corrosion or cracks.

IDTs made from the piezoelectric polymer PVDF have been studied at Imperial College; their basic construction and operation have been described elsewhere [6–9]. PVDF has been used as it is easy to work with, flexible and low cost, but it has the disadvantage that it is a relatively weak piezoelectric material compared with piezo-ceramics. Hence, in the long term, PVDF may be superseded by piezo-ceramic platelet matrices [10] or 1-3 piezo-composites [11]. However, although the amplitude of the acoustic field from an IDT is affected by the materials and the construction of the IDT, the shape of the acoustic field is only affected by the IDT geometry, subject to certain criteria being satisfied that will be discussed in Section 3.

IDTs made from 110 μm thick PVDF are designed to be permanently bonded at fixed locations on metallic (usually steel or aluminium) plates, into which they transmit and receive Lamb waves with a frequency–thickness product of around 1.3–1.4MHz mm. This frequency–thickness product is used as it corresponds to the maximum group velocity of the A_0 Lamb wave mode [8]. The PVDF that has been used (supplied from AMP, Harrisburg, USA) is supplied with thin (< 5μm) silver ink electrodes printed on both sides. If it is bonded to a structure in this form, the frequency response exhibits a peak at around 3.5MHz, and, below 3MHz, its sensitivity becomes too poor to be used in practical applications. This lower frequency limit therefore imposes an upper limit of approximately 0.4mm on the thickness of the plate that can be inspected using the A_0 Lamb wave mode. To transmit and receive this mode in thicker plates, the operating frequency must be reduced. This is achieved by removing one of the silver ink electrodes and replacing it with a 50μm thick copper electrode printed on poly-amide (i.e. printed circuit board material) that is bonded, copper side downwards, onto the PVDF. This reduces the minimum operating frequency of the PVDF to around 0.75MHz and, hence, imposes the current upper limit on plate thickness of approximately 1.8mm.

Fig. 1 shows a schematic diagram of a very simple PVDF IDT transmitting Lamb waves into a plate (the poly-amide layer is omitted for clarity in the Figure). The electrode pattern printed on the poly-amide con-

IEE Proceedings online no. 19982213

Paper first received 20th January and in revised form 5th April 1998

The authors are with the NDT Laboratory, Department of Mechanical Engineering, Imperial College, Exhibition Road, London SW7 2BX, UK

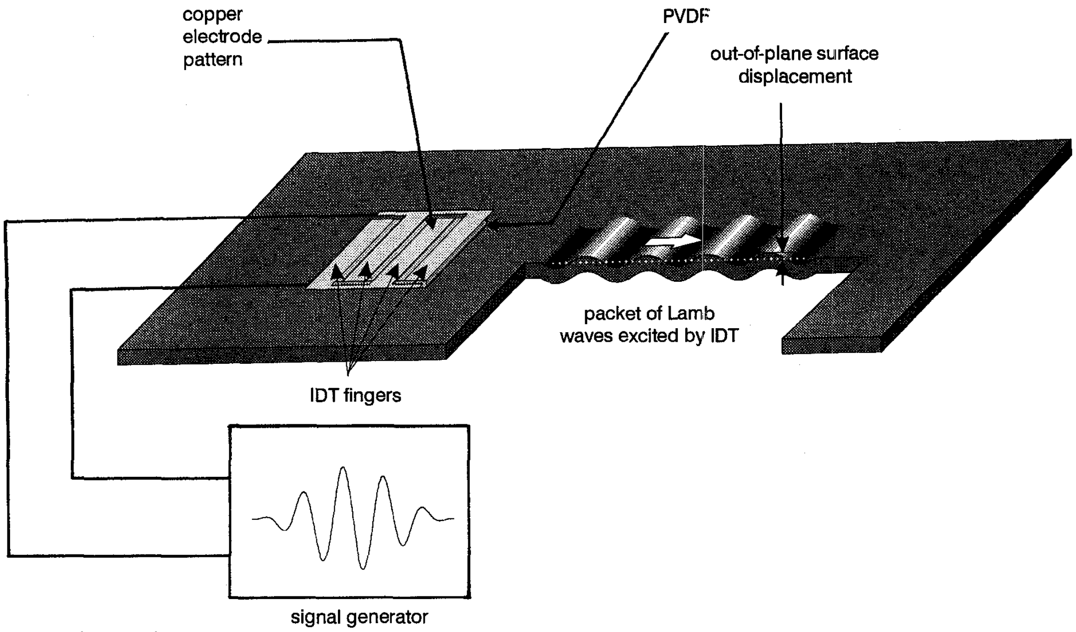

Fig. 1 *Generic features of simple PVDF IDT transmitting Lamb waves into plate structure*

sists of parallel strips, which are referred to as fingers and of which there are usually two sets. With two sets of fingers, the spacing between the centres of adjacent fingers is made equal to half the wavelength of the Lamb wave mode that the IDT is designed to transmit or receive. When the two sets of fingers are excited in anti-phase, a spatially harmonic stress distribution is set up on the surface of the plate beneath the transducer, the wavelength of which determines which Lamb wave mode is excited. More details on the construction of PVDF IDTs can be found in [7, 8].

The strength of the acoustic field that an IDT generates at a particular point in a plate is defined in this paper as the amplitude of the out-of-plane surface displacement at that point. For a PVDF IDT, the amplitude of these surface displacements is usually of the order of 1–10nm, whereas, for prototype IDTs made from piezoceramic–epoxy matrices [10], the amplitude is approximately one order of magnitude greater.

The IDTs described in this paper are not excited with continuous waves, but instead they are excited with short tonebursts, typically with 5–20 cycles, and they generate packets of Lamb wave energy that propagate into the plate away from the transducer. Thus, the acoustic field is continuously changing with respect to time and is not the static entity that its name suggests. However, for practical purposes, the strength of the acoustic field at a point on a plate is taken as being the maximum amplitude of surface displacement (the displacement being a function of time) that occurs at that point. This is measured experimentally by taking the maximum amplitude in a time trace received from a point transducer at the measurement location.

2 Interdigital transducers to produce different acoustic fields

PVDF IDTs are designed to transmit Lamb waves into plate structures and receive Lamb waves reflected from features in the structure, including defects. One possible IDT design could be completely axi-symmetric and would thus transmit and receive Lamb wave energy equally in all directions. However, some directionality in the acoustic field of an IDT is desirable from the point of view of locating defects. Experimental results from two types of design that produce directional acoustic fields are presented in this Section, and their relative merits are described.

2.1 Straight-finger interdigital transducers

An IDT with straight fingers is the Lamb wave analogue of a conventional plane transducer for transmitting longitudinal bulk waves. A well-designed straight-finger IDT will generate a straight collimated beam of Lamb waves that exhibits minimal divergence and can therefore propagate reasonably long distances in a free plate.

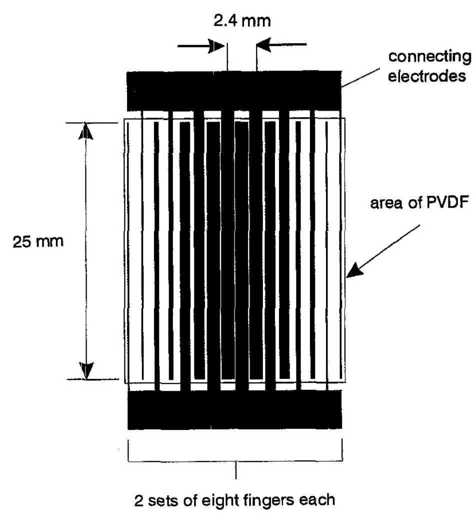

Fig. 2 *Geometry of typical straight finger IDT*
The finger sets are driven in anti-phase

The geometry of a particular straight-finger IDT is shown in Fig. 2. When bonded to a 1.2mm thick steel plate and excited with a toneburst at 1.1MHz, this IDT generates two packets of the A_0 Lamb wave mode that propagate out from either side of the transducer (all IDTs described in this paper are bi-directional, although uni-directionality has been achieved using three- or four-phase driving systems, an example of which is given in [12]).

To measure the acoustic field, the experimental set up shown in Fig. 3 was used. A specially constructed combined unit, incorporating a function generator and a power amplifier with a differential output [8], was used to drive the two sets of fingers of the IDT in anti-phase. The strength of the acoustic field in front of the IDT was measured at the locations shown in Fig. 3, to obtain three cross-sections through the acoustic field. The strength of the acoustic field was measured using a conical acoustic emission transducer (of a type similar to that described in [13]), connected through a low-noise charge amplifier to a digital oscilloscope. The conical transducer had a 1mm diameter flat tip, which was less than half the wavelength of the Lamb waves being investigated. After averaging 100 time signals at each point, the peak amplitude of the averaged time signal was measured. The resulting beam cross-sections are plotted in Fig. 4.

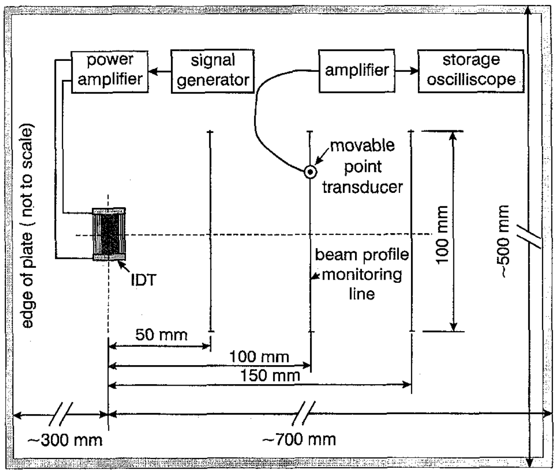

Fig.3 *Experimental set-up for measuring cross-sections through acoustic field for IDT shown in Fig. 2*

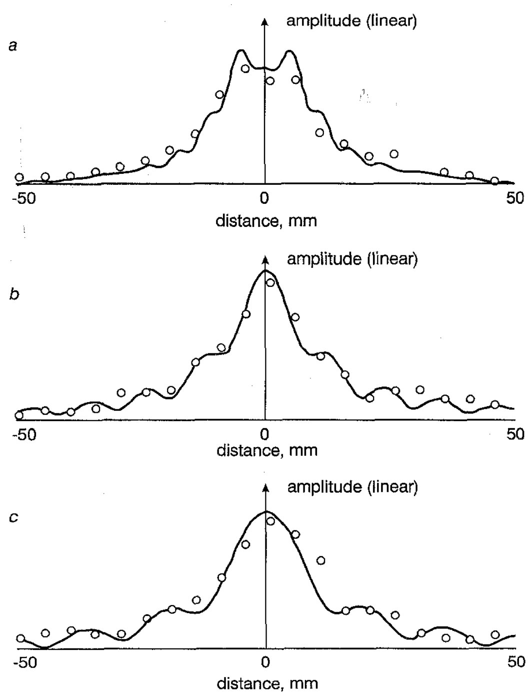

Fig.4 *Experimentally measured cross-section through acoustic field for IDT shown in Fig. 2 at (a) 50, (b) 100 and (c) 150mm*
○ experimental measurements
—— results predicted by Huygens' model

As can be seen from Fig. 4, the width of the main lobe of the beam remains fairly constant in all three cross-sections, indicating a collimated beam. The model results shown in the Figure are discussed in Section 3.

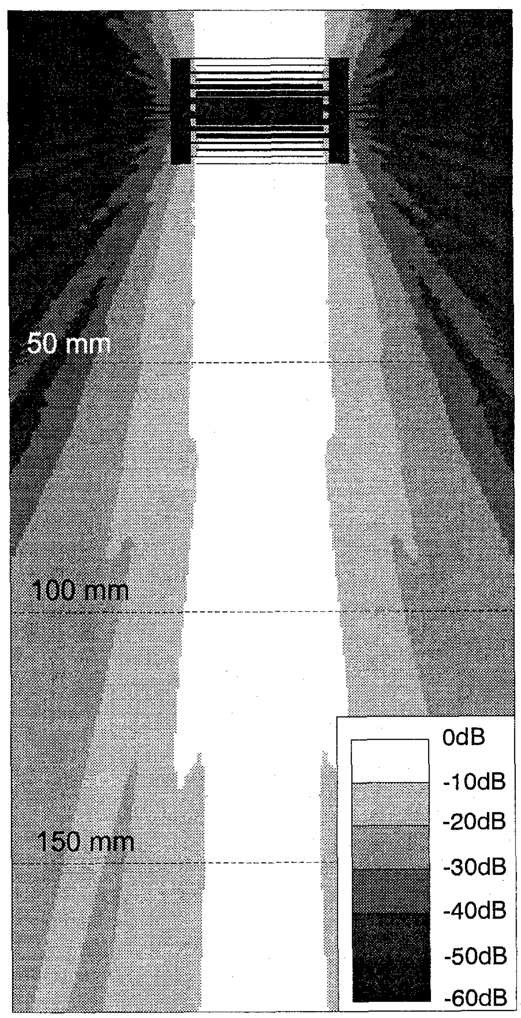

Fig.5 *Overall acoustic field for IDT shown in Fig. 2 predicted using Huygens' model*

2.2 Curved-finger interdigital transducers

The straight-finger IDT described above can transmit waves over considerable distances owing to its collimated beam, but this attribute unfortunately means that it is only sensitive to defects along a fairly narrow straight line in front of it. To monitor a reasonable area of structure using a straight-finger IDT would require a very wide transducer. Attention is now turned to curved-finger IDTs that can generate divergent (i.e. defocused) beams. Although the amplitude of a divergent beam must necessarily decrease more rapidly with distance than that of a collimated beam, the divergent beam enables a pie-slice shaped area of a plate to be inspected from a single transducer.

Once again, a specific curved-finger IDT is considered as an example, the geometry of which is shown in Fig. 6. This particular curved-finger IDT is actually one of a set of six identical IDTs that were fabricated as a single unit (as indicated in Fig. 6), the intention being that the six IDTs together would have a 360° 'field of vision' about themselves.

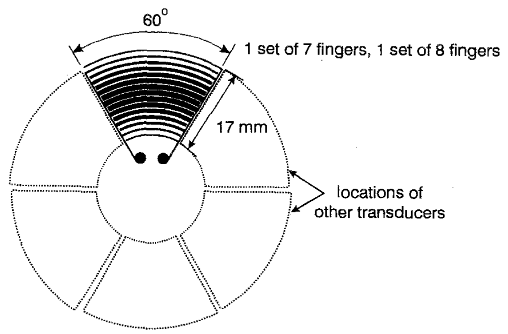

Fig. 6 *Geometry of typical curved-finger IDT*

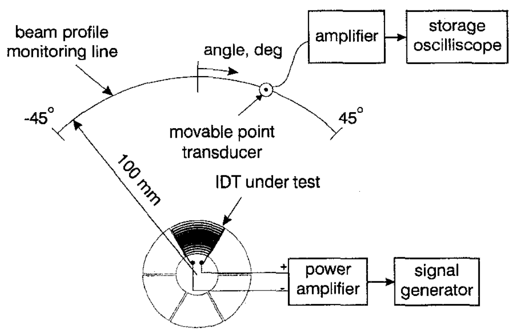

Fig. 7 *Experimental set-up for measuring angular cross-section through acoustic field for IDT shown in Fig. 6*

A cross-section through the acoustic field from this IDT was measured using the same technique as described above, except that, in this case, the cross-section was taken on a circular arc, concentric with the fingers of the IDT, as shown in Fig. 7. Later work, using the model described in Section 3, has shown that an angular section through the field from a curved-finger IDT is almost completely independent of the radius at which the cross-section is taken. The experimentally measured angular cross-section for this particular IDT is plotted in Fig. 8.

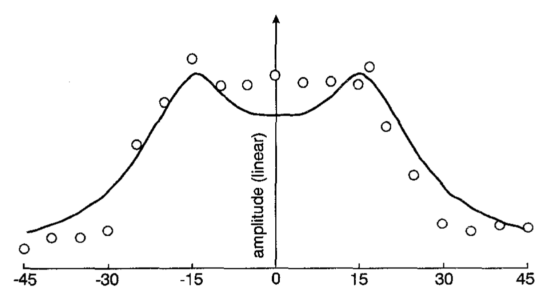

Fig. 8 *Angular acoustic field cross-section for IDT shown in Fig. 6 at location shown in Fig. 7*
○ experimental measurements
—— Huygens' model predictions

As can be seen from Fig. 8, the IDT produces a field that is reasonably flat over the angular range from −20° to 20°. This is close to an ideal divergent acoustic field for inspecting a 40° sector of plate. Unfortunately, there were only six IDTs in the circular configuration shown in Fig. 6, and, hence, it would be desirable for each IDT to be able to monitor a 60° sector of the plate. This circular configuration is therefore inadequate for the task. Thus, it can be seen that some method of predicting the acoustic field for a particular geometry of IDT is required for the design to be optimised, so that the acoustic field will cover the required area of the plate.

3 Modelling acoustic field from interdigital transducers

The preceding Section has shown practical examples of the types of acoustic field that IDTs can be used to create. The next issue to be addressed is how to predict the acoustic field for a particular geometry of IDT. It has already been shown [8] that satisfactory agreement with experimental measurements of the acoustic field from an IDT can be obtained using a time marching finite-element (FE) model of the plate, representing the action of the fingers of the IDT by forces applied along lines on the surface of the plate. Unfortunately, such an FE model takes several days to run, even for the simplest cases, and is therefore not a practical IDT design tool.

3.1 Huygens' model for interdigital transducers generating Lamb waves

In theory, the acoustic field could be predicted analytically, and this has been done for surface acoustic wave transducers used in signal processing applications using normal mode expansions [14]. Work is currently in progress to use a similar method for Lamb wave IDTs, but this method is likely to be very complex, owing to the three-dimensional nature of the problem. The problem can be simplified if the presence of the transducer does not significantly reflect, scatter or otherwise affect the characteristics of Lamb waves passing beneath it. This will be the case for IDTs that have a small mass per unit area compared with that of the plate, or that are weakly coupled to it. Both of these criteria are reasonably well satisfied by the PVDF IDTs that are considered here. The action of the IDT can therefore be modelled by a series of normal forces applied to the plate at the finger positions, as was assumed for the FE model described in [8].

The field from a time-harmonic, axi-symmetric distribution of stress can be calculated exactly [15] and consists of circular crested Lamb waves that propagate outwards from the source in an axi-symmetric fashion. From this, the out-of-plane surface displacement field (i.e. acoustic field) u_z, due to a time-harmonic, normal point force is obtained

$$u_z = F_0 \sum_m E^{(m)}(f) H_0^{(1)}\left(\frac{2\pi f}{v_{ph}^{(m)}(f)} r\right) e^{-2i\pi f t} \quad (1)$$

where t is the time, r is the distance from the source, f is the frequency of excitation and F_0 is the amplitude of excitation. The summation sign indicates that the field is a superposition of contributions from all the modes m that can exist at the excitation frequency. Each mode has a phase velocity $v_{ph}^{(m)}$ and an excitability $E^{(m)}$, which are both functions of frequency. The excitability of a mode is largely governed by the quantity of out-of-plane surface displacement in its mode shape. Modes with a large amount of out-of-plane surface displacement couple well to the action of normal forces applied to the surface of a plate and therefore are more excitable.

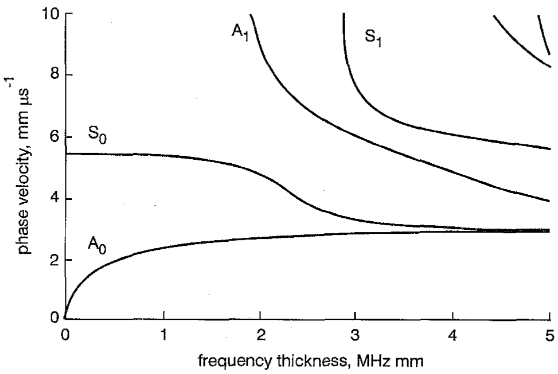

Fig. 9 *Phase velocity curves for circular crested Lamb waves in aluminium plate*

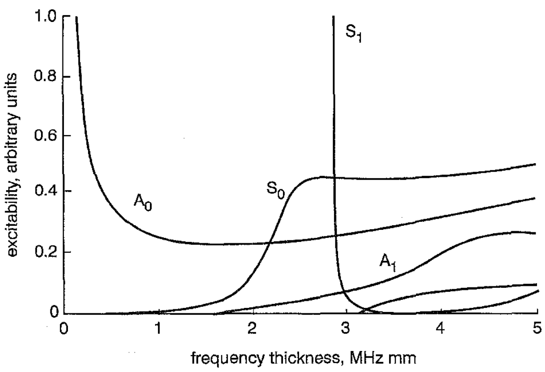

Fig. 10 *Excitability curves for circular crested Lamb waves in aluminium plate*

The phase velocity and excitability curves are plotted for the case of an aluminium plate in Figs. 9 and 10, respectively. The phase velocity curves in Fig. 9, which are used in eqn. 1 to represent circular crested Lamb waves, are in fact the same as those for straight crested Lamb waves [15]. The difference between the two cases is that for circular crested Lamb waves, the spatial variation is given by the Hankel function $H_0^{(1)}$ in eqn. 1, whereas, in the case of straight crested Lamb waves, the spatial variation is a harmonic function of distance.

The acoustic field due to the application of harmonic normal surface stress over any area can be calculated by considering the area as a series of elements, each of which is modelled as a point source. Hence, by integrating the fields from all the elements, the total acoustic field can be obtained. In general, the integration cannot be solved analytically, and, hence, it must be calculated numerically by performing a complex summation of the acoustic fields from a number of point sources, each of which represents a finite-sized element of the IDT. The size of element that is required for the solution to converge has been investigated. This has shown that a finger of an IDT can be accurately modelled by using a single row of point sources (i.e. elements), and that the separation of the point sources (i.e. the length of each element) must not be greater than a quarter of the wavelength of the shortest Lamb wave in the system. This is the basis of what has been termed the Huygens' model for IDTs, because the principle of the superposition is the same as that which he used for optical fields and which can also be used to calculate the field from a conventional plane transducer [16]. By treating the amplitudes of the applied surface stresses as complex quantities, the model can also be used for cases where there is more than one phase of excitation.

The model described above is for continuous single-frequency excitation, whereas, in practice, IDTs are excited with tonebursts of finite duration and bandwidth. The Huygens' model can easily be expanded to model toneburst excitation by modelling each frequency component of the toneburst separately and then recombining the results by superposition. It should be noted that the acoustic fields calculated for toneburst and continuous excitation are not the same, although, in practice, the continuous-excitation model represents a very reasonable approximation to the toneburst excitation solution. The reason for the difference between the two cases is described below.

The shape of the acoustic field from the entire IDT is determined by constructive and destructive interference taking place between the acoustic fields from each of the point sources. When excited continuously, the energy in the acoustic field from a single point source is distributed over the entire plate at all instants in time. Therefore interference occurs between the fields from any two points, regardless of their spatial separation. However, when toneburst excitation is used, the energy in the acoustic field from a single point source at a particular instant in time is contained in an annular region centred on that point. The width of the annular region is the spatial length of the toneburst of Lamb waves. Hence, interference between the fields from two point sources only occurs where the annular regions of the acoustic fields from each point intersect. If the separation of the two points is small compared with the spatial length of the toneburst, then the majority of both annular regions will intersect, and the interference pattern in this region will be very similar to that which would be obtained if continuous excitation was used. Hence, if an IDT has dimensions that are small compared with the spatial length of the toneburst with which it is excited, the acoustic field that is generated will be approximately the same as if the IDT were excited continuously.

The major assumption in the Huygens' model is that the field from each point source representing an IDT is unaffected by the presence of the rest of the transducer. This assumption is known not to be correct, as the Lamb waves propagating under an IDT are subject to attenuation caused by energy leaking from the plate into the IDT and perhaps some scattering. However, validation studies have indicated that this does not significantly affect the overall acoustic field. It should also be noted that the FE model that was used previously made exactly the same assumptions. The Huygens' model has been validated against the FE model for several cases, and excellent agreement has been obtained. The time taken to compute the complete acoustic field from an IDT using the Huygens' model takes in the order of minutes, rather than the days taken by the FE model. Hence, the Huygens' model is viable for use as an interactive design tool.

3.2 Implementation of Huygens' model in software

The Huygens' model described above has been implemented in a Microsoft Windows application for use on PC computers. The model is in two parts: the first is concerned with predicting the acoustic field from a point source, and the second performs the Huygens' superposition to obtain the field from an IDT.

In the first part of the program, the required inputs are the excitation signal as a function of time and the Lamb wave dispersion curves from which the excitability curves are also calculated. The excitation signal can be either of finite length, such as a toneburst, or a continuous sine wave. The program then calculates a matrix of complex surface displacements, where the rows represent time and the columns represent distance. Thus each row in the matrix is the surface displacement as a function of distance from the source at a particular instant in time. Complex values for surface displacement are calculated, where the real part is the instantaneous physical displacement (and is therefore spatially harmonic), the imaginary part is shifted by 90° with respect to the real part, and the amplitude of the displacement thus gives the spatial envelope over the individual wave-crests. If the input is a continuous wave, then the amplitude of the displacements is constant at all times, and only a single row in the matrix is necessary.

The second part of the program takes the matrix of surface displacements as an input, together with a file specifying the location of point sources required to model the IDT. The acoustic field at a particular point, at an instant in time, due to a single point source, is obtained from the matrix of surface displacements. The total acoustic field strength at a point can then be calculated by addition of the surface displacements contributed by each of the sources. Using this technique, an image of the overall acoustic field can be obtained by calculating the acoustic field strength at locations arranged in a raster pattern. Alternatively, the acoustic field strength can be calculated at points along arcs or straight lines, to obtain cross-sections through the overall field.

3.3 Comparison of results of Huygens' model with experimental measurements

Consider the straight-finger IDT described in Section 2 and shown in Fig. 2. The acoustic field was calculated using the Huygens' model, and the result is plotted in Fig. 5. The well-collimated beam that was found from the experimental measurements is clearly evident in this plot. Cross-sections through the field calculated using the Huygens' model are superimposed on the experimentally measured cross-sections in Fig. 4. As can be seen, good agreement is obtained. The angular cross-section predicted by the Huygens' model for the curved-finger IDT described in Section 2 is also shown with the experimental results in Fig. 8. Again, reasonable agreement is obtained in terms of the overall angular extent of the field, although the exact agreement at the edges of the main beam is not as good. These discrepancies are thought to result from inconsistencies introduced when bonding the IDT to the plate.

4 Application of Huygens' model to design of interdigital transducers

It is instructive to use the Huygens' modelling software to obtain some general guidelines for the design of IDTs. In these investigations, all dimensions are specified in terms of the wavelength of the Lamb waves that the IDT is designed to excite.

4.1 Straight-finger interdigital transducers

It has been noted that the main use for straight-finger IDTs is to generate collimated beams. It is therefore desirable to obtain an expression for the beam divergence angle for a straight-finger transducer, in much the same way as one can be found for a plane bulk wave transducer [17]. For simplicity, a single-finger IDT is considered first; the effect of adding multiple fingers will be addressed later.

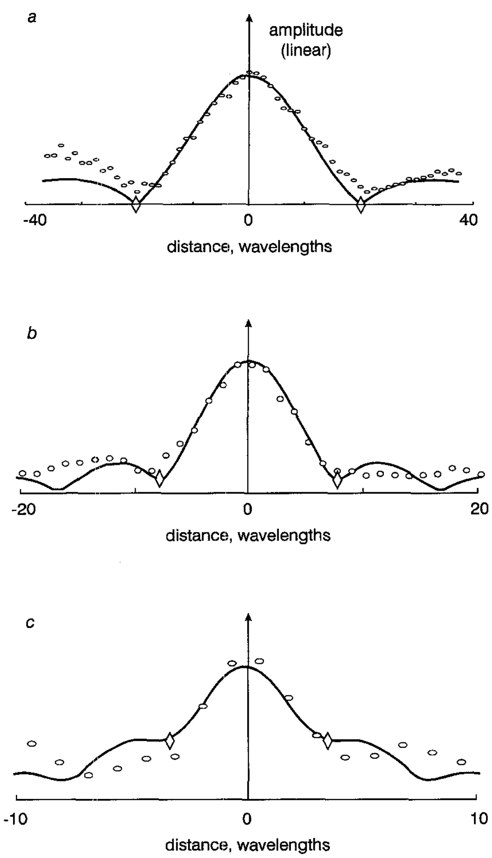

Fig. 11 *Cross-sections through fields for fingers of length (a) 2, (b) 5 and (c) 10 wavelengths*
The diamonds show the locations of the first minima on either side of the main lobe of the beam
○ experimental results
—— Huygens' model

The beam divergence angle is defined in the same way as for a bulk wave transducer, i.e. the angle at which the first minima in the amplitude of the field on either side of the main lobe of the beam diverge (such minima are marked in Fig. 11. Using the Huygens' model, the beam divergence angle was calculated for fingers in the range 1–25 wavelengths long. The results are plotted in Fig. 12, together with some example beam cross-sections and experimental measurements in Fig. 11. The fitted curve shown in Fig. 12 is given by the equation

$$\gamma = \sin^{-1}\left(\frac{\lambda}{l}\right) \qquad (2)$$

where γ is the beam divergence angle, l is the length of the finger, and λ is the wavelength. This is very similar to the corresponding expression for a bulk wave transducer [17] of diameter l, where the beam divergence angle is given by $\sin^{-1}(1.2\lambda/l)$, the difference being thought to arise from the IDT system being for two-dimensional wave propagation, whereas the bulk wave transducer system is three-dimensional. From Fig. 12, it can be seen that, for a reasonably non-divergent beam, the finger length should be 10 or more wavelengths.

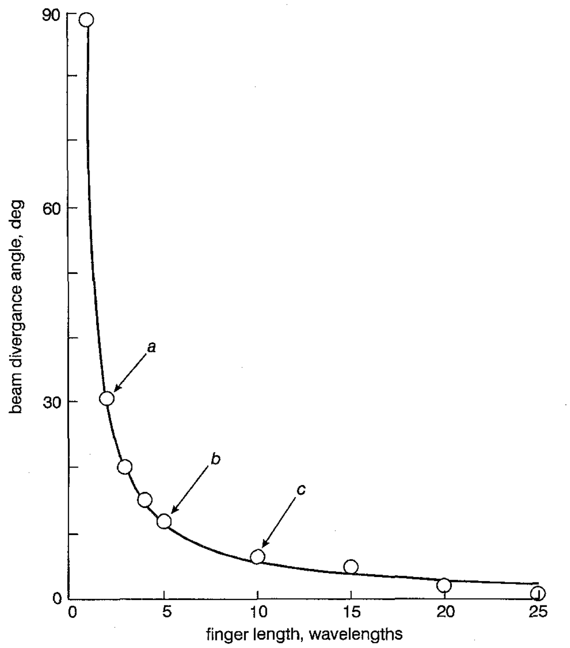

Fig. 12 *Predicted beam divergence as function of finger length for IDT with single straight finger*
a, *b* and *c* correspond to Figs. 11*a*, 11*b* and 11*c*, respectively
○ measured from Huygens model
—— fitted curve $\sin^{-1}(\lambda/l)$

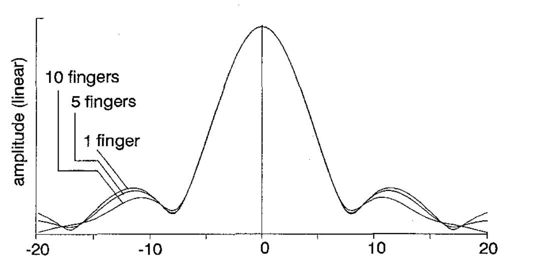

Fig. 13 *Angular cross-sections through acoustic field from straight-finger IDT with 1, 5 and 10 fingers*

The effect of adding more fingers to an IDT was investigated using the Huygens' model, and the results are shown in Fig. 13. This shows cross-sections, taken at a distance of 40 wavelengths, through the acoustic field of a straight-finger IDT (with a finger length of 10 wavelengths) with different numbers of fingers. The sections are all normalised by their peak amplitude, as the absolute amplitude is approximately proportional to the number of fingers. It can be seen that, perhaps surprisingly, the number of fingers makes little or no difference to the width of the main lobe of the field and only starts to have noticeable effects at the sides, where the amplitude is some 20dB below the peak amplitude of the field. From this it can be concluded that the number of fingers in a straight-finger IDT does not affect the relationship between the finger length and the beam divergence angle given in eqn. 2. The advantage of using multiple fingers is to increase the overall acoustic power entering the structure and to improve the wavelength selectivity of the IDT [8].

4.2 Curved-finger interdigital transducers

For a curved-finger IDT, general trends are more complicated to determine, as there are more design parameters than for a straight-finger IDT. Furthermore, the definition of a measurable quantity with which to compare different acoustic fields is somewhat difficult.

As a starting point, it will be assumed that the goal when designing a curved-finger IDT is to produce one that generates a field that diverges at the same angle as that subtended by the fingers (hereafter referred to as the angle of the IDT). This ideal field will, at a particular distance from the geometric centre of the IDT, have a constant amplitude within the angle of the IDT and zero amplitude elsewhere. In the studies presented here, only IDTs with concentric fingers, which all subtend the same angle about their common centre, are considered. This reduces the number of design parameters to be investigated to three: the angle subtended by the fingers (the angle of the IDT), the radius (which is taken as the mean of the innermost and outermost radii for IDTs with more than one finger) and the number of fingers. The effects of radius and angle on the beam from an IDT with a single curved finger are described below. The effect of multiple fingers is currently under investigation.

Consider an IDT with a single curved finger of angle 90°. Angular beam cross-sections predicted using the Huygens' model are plotted for several different radii of finger in Fig. 14, all cross-sections being taken at a radius of 30 wavelengths. The energy at a point in the acoustic field is proportional to the square of the amplitude of the acoustic field at that point. Integrating the energy in the acoustic field over a 180° cross-section enables the total energy to be found. The amplitude of an ideal beam containing the same total energy can then be calculated. The ideal beams are plotted with lighter lines in Fig. 14. It can be seen that the general trend is that the actual beam becomes closer to the ideal beam as the radius is increased. As this occurs, the cut-offs on either side of the main beam become sharper, and the fluctuations within the main beam become shallower and more numerous.

Fig. 15 shows some of the results from a similar study on an IDT with a single curved finger, except that, in this case, the radius of the finger was kept constant (and equal to 5 wavelengths), while its angle was varied. From these graphs, it can be seen that the field is closest to the ideal field when the angle is large, and deteriorates as the angle is reduced.

For a selection of the IDT geometries shown in Figs. 14 and 15, experimental measurements have been made using a similar technique to that described in Section 2, and the results are plotted on the Figures. Once again,

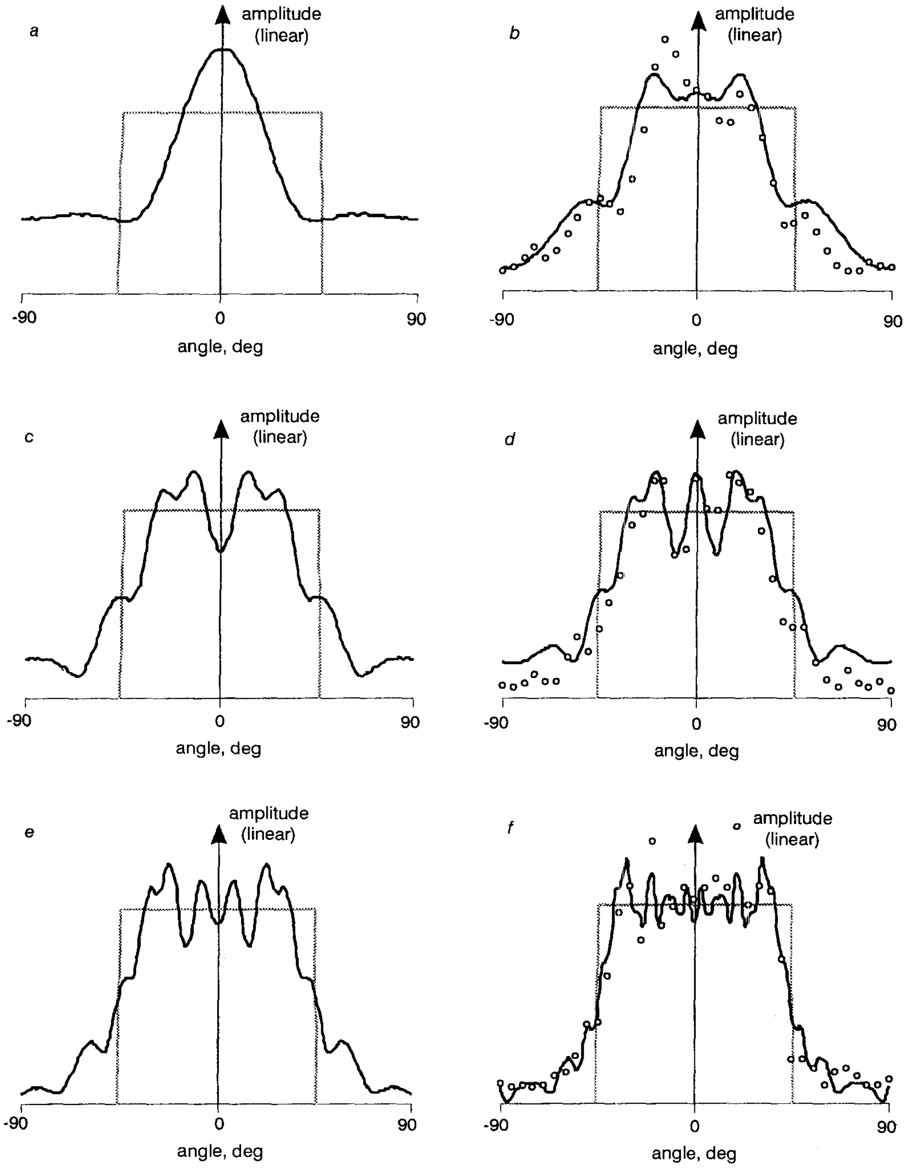

Fig. 14 *Predicted angular cross-sections through acoustic field from IDT with single curved finger of angle 90° as radius of finger is increased from (a) 1, (b) 2, (c) 3, (d) 4, (e) 5 and (f) 10 wavelengths*
Cross-sections through the ideal fields are shown with lighter lines and where applicable, experimental measurements are shown by black circles

good agreement is achieved between experimental measurements and predictions made using the Huygens' model.

By integrating the discrepancy between the energy in the beam profile predicted by the Huygens' model and the ideal beam profile over the angular range of each cross section, and dividing this by the total energy in the beam, a numerical measure of the beam quality can be obtained for any IDT, which enables a quantitative comparison to be made between the acoustic fields of any curved-finger IDTs.

For a given angle of transducer with a single finger, the beam quality is a function of the radius of the finger, as shown in Fig. 16 for the case of a single 60° finger. It can be seen that, if the radius is large, the beam quality increases approximately monotonically with radius, as the first study suggested. However, if the radius is small, the beam quality fluctuates both up and down, the amplitude of the fluctuations increasing as the radius is reduced. At some critical radius, the beam quality reaches a final peak before continuously decreasing as the radius is reduced to zero. This critical radius has been found to occur when the distance between the centre of a chord joining the ends of the finger and the centre of the finger equals half a wavelength. Below this radius, a curved-finger IDT behaves more like a straight-finger one. This critical radius gives the absolute minimum size of a curved-finger IDT necessary to produce a divergent beam.

Plotting contours of constant beam quality on a graph of radius against angle for an IDT with a single curved finger enables the general trends from the above studies to be visualised, and this is shown in Fig. 17. The critical radius is plotted as a function of angle in Fig. 17, and the region where the beam quality is a rapidly fluctuating function of radius is also indicated, the upper bound of this region being set at four times the critical radius.

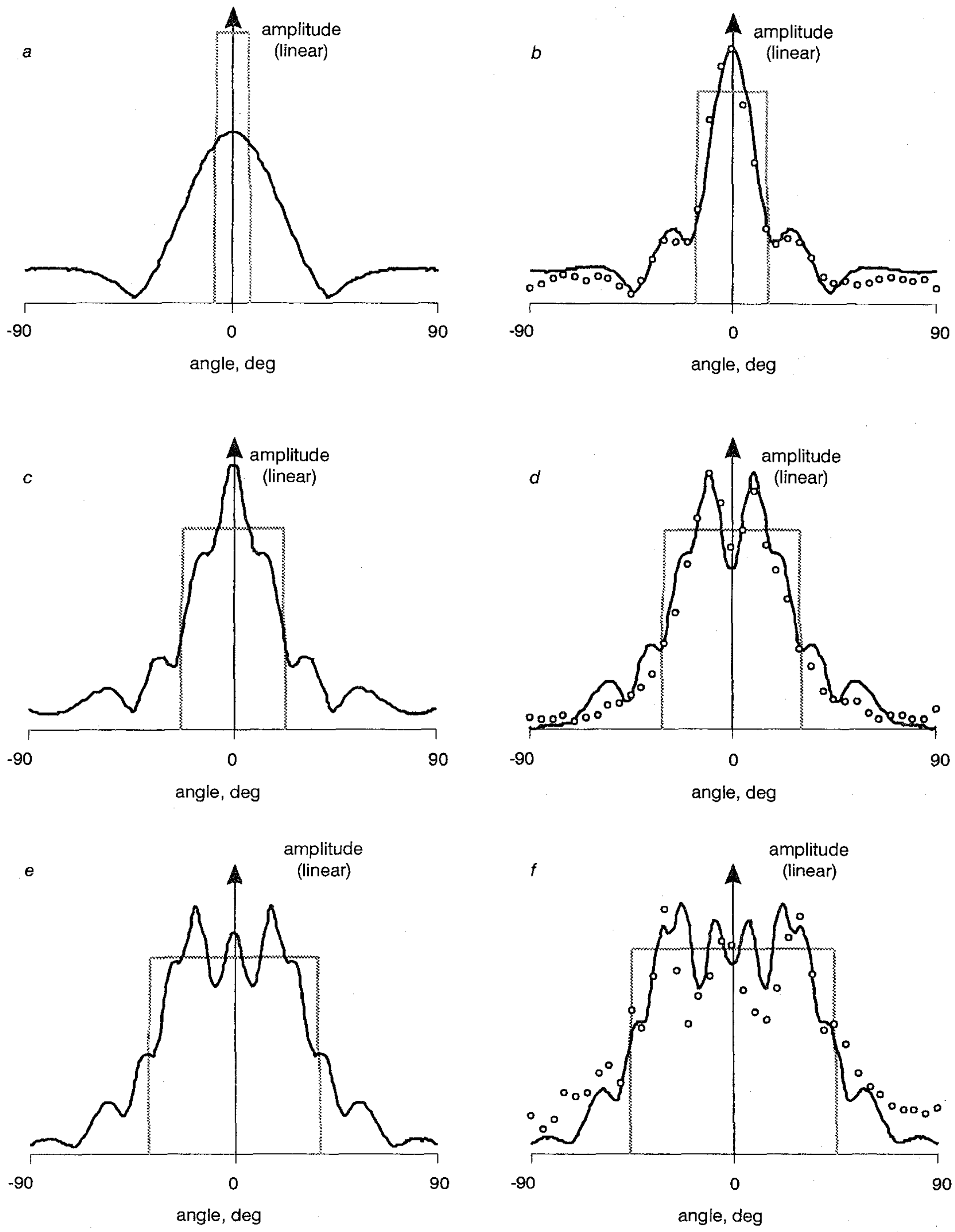

Fig. 15 *Predicted angular cross-sections through acoustic field from IDT with single curved finger of radius 5 wavelengths as angle of finger is increased from (a) 15°, (b) 30°, (c) 45°, (d) 60°, (e) 75° and (f) 90°*
Cross-sections through the ideal fields are shown with lighter lines and where applicable, experimental measurements are shown by black circles

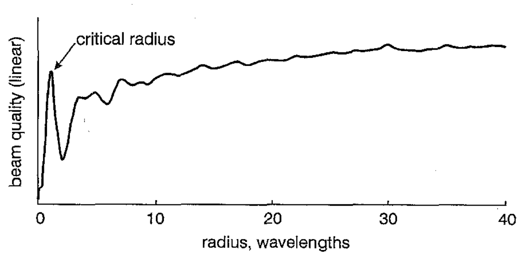

Fig. 16 *Predicted beam quality as function of radius for single 60° finger, showing critical radius*

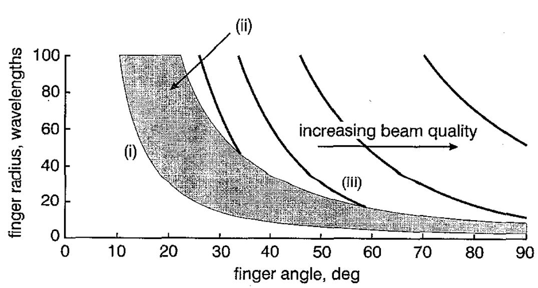

Fig. 17 *Radius and angle combinations required to produce particular beam qualities for IDT with single curved finger*
The critical radius is also plotted
(i) Minimum critical radius; (ii) region of large fluctuations in beam quality; (iii) contours of constant beam quality

The minimum radius of a curved-finger IDT that is necessary to inspect a sector of a structure over a particular angle is of considerable interest, as the radius determines the overall size of the IDT. Initial studies on the effect of using more fingers suggest that the effect is a smoothing out of the beam profile that generally results in an improvement in the beam quality.

This effect is most apparent when the mean radius of the IDT is small. This is a useful result, as it will enable smaller IDTs to be constructed without the beam quality being compromised.

5 Conclusions

PVDF IDTs have been built that transmit and receive Lamb waves in thin structures. By tailoring the design of such IDTs, different shapes of acoustic field can be produced in the structure. Modelling software based on Huygens' principle has been developed that allows the acoustic field from an IDT to be predicted, and results from this model compare well with experiments. As the model is very fast to run, it can be used as an interactive design tool for IDTs.

Preliminary results from the model have been used to elucidate general relationships between IDT geometry and resulting acoustic fields. It has been shown that, for a straight-finger IDT producing a collimated beam, a relationship between the beam divergence angle and the width of the IDT exists similar to that which exists for conventional bulk wave transducers. It has also been demonstrated that increasing the number of fingers in a straight-finger IDT does not significantly affect the shape of the acoustic field, although it does allow greater transducer sensitivity and modal selectivity [8]. For curved-fingered IDTs producing divergent beams, it has been found that, for a given angle of divergence, there is a minimum radius for the transducer to be effective, and that this minimum radius decreases as the angle increases.

6 Acknowledgments

The authors wish to thank Roger Dalton for taking the acoustic field measurements presented in Section 2, and Richard Monkhouse for his invaluable assistance throughout this work.

7 References

1 WORLTON, D.C.: 'Ultrasonic testing with Lamb waves', *Nondestruct. Test.*, 1957, pp. 218–222

2 ALLEYNE, D.N., and CAWLEY, P.: 'The interaction of Lamb waves with defects', *IEEE Trans. Ultrason., Ferroelectr. Freq. Control*, 1992, **39**, (3), pp. 381–397

3 VIKTOROV, I.A.: 'Rayleigh and Lamb waves: Physical theory and applications' (Plenum Press, 1967)

4 ALERS, G.A., and BURNS, L.R.: 'EMAT designs for special applications', *Mater. Eval.*, 1987, **45**, pp. 1184–1189

5 JIA, X.: 'Modal analysis of Lamb wave generation in elastic plates by liquid wedge transducers', *J. Acoust. Soc. Am.*, 1997, **101**, (2), pp. 834–842

6 WILCOX, P.D., MONKHOUSE, R.S.C., CAWLEY, P., LOWE, M.J.S., and AULD, B.A.: 'Development of a computer model for an ultrasonic polymer film transducer system', *NDT & E Int.*, 1998, **31**, (1), pp. 51–64

7 MONKHOUSE, R.S.C., WILCOX, P.D., and CAWLEY, P.: 'Flexible interdigital PVDF Lamb wave transducers for the development of smart structures' *in* CHIMENTI, D.E., and THOMPSON, D.O. (Eds.): 'Annual review of progress in quantitative NDE, **16A**' (Plenum Press, New York, 1997), pp.877–884

8 MONKHOUSE, R.S.C., WILCOX, P.D., and CAWLEY, P.: 'Flexible interdigital PVDF transducers for the generation of Lamb waves in structures', *Ultrasonics*, 1997, **35**, pp. 489–498

9 WILCOX, P.D., CASTAINGS, M., MONKHOUSE, R.S.C., CAWLEY, P., and LOWE, M.J.S.: 'An example of the use of interdigital PVDF transducers to generate and receive a high order Lamb wave mode in a pipe' *in* CHIMENTI, D.E., and THOMPSON, D.O. (Eds.): 'Annual review of progress in quantitative NDE, **16A**' (Plenum Press, New York, 1997), pp.919–926

10 GACHAGAN, A., REYNOLDS, P., HAYWARD, G., and McNAB, A.: 'Construction and evaluation of a new generation of flexible ultrasonic transducers'. Proceedings of IEEE *Ultrasonics* symposium, 1996, pp. 853–856

11 TRAN-HUU-HUE, L.P., LEVASSORT, F., LETHIECQ, M., CERTON, D., and PATAT, F.: 'Characterisation of the piezoelectric and dielectric relaxation parameters of 0-3 composites and PVDF materials in the thickness mode', *Ultrasonics*, 1997, **35**, pp. 317–324

12 WILCOX, P.D., MONKHOUSE, R.S.C., LOWE, M.J.S. and CAWLEY, P.: 'The use of Huygens' principle to predict the acoustic field from inter-digital Lamb wave transducers' *in* CHIMENTI, D.E., and THOMPSON, D.O. (Eds.): 'Annual review of progress in quantitative NDE, **17**' (Plenum Press, 1998)

13 GREENSPAN, M.: 'The NBS conical transducer: analysis', *J. Acoust. Soc. Am.*, 1987, **81**, (1), pp. 173–183

14 AULD, B.A.: 'Acoustic fields and waves in solids' (Krieger Publishing Company,1990)

15 DITRI, J.J., PILARSKI, A., ROSE, J.L., and PAVLAKOVIC, B.: 'Generation of guided waves in a plate by axisymmetric normal surface loading', *in* CHIMENTI, D.E., and THOMPSON, D.O. (Eds.): 'Annual review of progress in quantitative NDE, **12A**' (Plenum Press, New York, 1994)

16 KRAUTKRAMER, J. and KRAUTKRAMER, H.: 'Ultrasonic testing of materials' (Springer-Verlag Berlin Heidelberg New York, 1983)

17 SILK, M.G.: 'Ultrasonic transducers for nondestructive testing' (Adam Hilger Ltd., 1984)